

Supporting information

Evaluation of a conceptual model for gas-particle partitioning of polycyclic aromatic hydrocarbons using poly-parameter linear free energy relationships

Pourya Shahpoury^{1*}, Gerhard Lammel^{1,2*}, Alexandre Albinet³, Aysun Sofuoğlu⁴, Yetkin Dumanoglu⁵, Sait C. Sofuoğlu^{4,6}, Zdeněk Wagner⁷, Vladimir Zdimal⁷

¹ Multiphase Chemistry Department, Max Planck Institute for Chemistry, Mainz, Germany

² Research Centre for Toxic Compounds in the Environment, Brno, Czech Republic

³ INERIS (Institut National de l'Environnement Industriel et des Risques), Verneuil-en-Halatte, France

⁴ Chemical Engineering Department, Izmir Institute of Technology, Urla, Turkey

⁵ Environmental Engineering Department, Dokuz Eylül University, Izmir, Turkey

⁶ Environmental Engineering Department, Izmir Institute of Technology, Urla, Turkey

⁷ Institute for Chemical Process Fundamentals, the Czech Academy of Sciences, Prague, Czech Republic

*Corresponding authors: Pourya Shahpoury; phone: +49 6131 305 7602;

Email: p.shahpoury@mpic.de; address: Hahn-Meitner-Weg-1, 55128 Mainz, Germany

Gerhard Lammel; phone: +49 6131 305 7601;

Email: g.lammel@mpic.de; address: Hahn-Meitner-Weg-1, 55128 Mainz, Germany

The supporting information consists of 30 pages including ten figures and six tables

Table of contents

S1 Sampling, chemical analysis and quality control for gas-particle partitioning data	4
Table S1 Estimated safe sampling volumes (m^3) in the gas phase and analyte concentrations (mean \pm standard deviation) in field blanks (G: gas phase; P: particulate phase)	7
S2 Junge-Pankow model	7
S3 Finizio and Dachs-Eisenreich models	8
S4 Methodology for ppLFER calculations	10
S5 Information on chemistry of organic phases considered for ppLFER model	11
Table S2 Abraham solute descriptors used for ppLFER calculations.....	14
Table S3 ppLFER system parameters	14
Table S4 Minimum, maximum, and median PAH particulate mass fractions (Θ ; unitless), ambient temperature (T; $^{\circ}\text{C}$), and PM sample compositions	15
Figure S1A PAH particulate mass fractions (Θ) as a function of temperature at Košetice	16
Figure S1B PAH particulate mass fractions (Θ) as a function of temperature at Grenoble.	17
Figure S1C PAH particulate mass fractions (Θ) as a function of temperature at Urla.....	18
S6 Model predictions	19
S6.1 ppLFER model predictions	19
Figure S2 Predicted versus experimental $\log K_P (\text{m}^3_{\text{air}} \text{g}^{-1}_{\text{PM}})$ for Košetice ($n = 56$), ppLFER model based on organic aerosol from Dübendorf autumn (A) and Berlin winter (B)	19
Figure S3 Predicted versus experimental $\log K_P (\text{m}^3_{\text{air}} \text{g}^{-1}_{\text{PM}})$ for Grenoble ($n = 114$), multi-phase ppLFER model using measured f_{WSOM} (Phase A) and $1 - f_{\text{WSOM}}$ (Phase B).....	20
Table S5 Root mean square errors and percentage of data points predicted within one order of magnitude accuracy (in parenthesis) for Grenoble dataset using a range of soot specific surface areas	20
S6.2 Multiphase ppLFER model predictions with substances other than PAHs	21
Figure S4 Predicted versus experimental $\log K_P (\text{m}^3_{\text{air}} \text{g}^{-1}_{\text{PM}})$ for furans at Košetice ($n = 50$), multi-phase ppLFER model.....	23
Figure S5 Partitioning constants ($\text{m}^3_{\text{air}} \text{g}^{-1}_{\text{PM}}$) predicted using multi-phase ppLFER and Finizio models versus observed values for 16 mono-aromatic compounds.....	23
S6.3 spLFER model predictions	24
Figure S6 Median c_J (Pa cm) calculated using experimental Θ , S , and p_L^0 (T) at Košetice	24
Figure S7 Median PM surface concentrations ($\text{cm}^2_{\text{surface}} \text{cm}^{-3}_{\text{air}}$) determined using PM number size distribution at Košetice	24

Table S6 Experimental c_j for individual PAHs	25
Figure S8 Predicted versus experimental $\log K_p$ ($\text{m}^3_{\text{air}} \text{g}^{-1}_{\text{PM}}$) for Košetice ($n = 150$), Junge-Pankow model.....	25
Figure S9 Predicted versus experimental $\log K_p$ ($\text{m}^3_{\text{air}} \text{g}^{-1}_{\text{PM}}$), Finizio and Dachs-Eisenreich models; $n = 46, 114,$ and 18 for Košetice, Grenoble, and Urla, respectively	26
Figure S10 Median contributions of absorption into organic matter and adsorption onto soot for Dachs-Eisenreich model	27
References	28

S1 Sampling, chemical analysis and quality control for gas-particle partitioning data

At Košetice, a total of 162 samples were collected every sixth day in 2012 and 2013, 108 samples using a Digitel DH-77 high-volume sampler mounted with 15-cm inner diameter (ID) quartz fiber filter (QFF) and two 10-cm ID polyurethane foam (PUF) plugs (12 cm total depth) over 24-hour periods, and 54 samples using a Graseby-Andersen PS-1 high-volume sampler fitted with 10.1-cm ID QFF and two 5.5-cm ID PUF plugs (10 cm total thickness) with collection time between 6 and 35 hours. At Grenoble, 122 samples were collected every third day in 2013 using a Digitel DA-80 high-volume sampler, each for a period of 24 hours. Particulate phase was collected on a 15-cm ID QFF, while gas phase was collected on a 10-cm ID PUF plug (7.5 cm thickness). At Urla, 22 day and night samples (12-hourly) were collected using a Thermo-Andersen GPS-11 high-volume sampler fitted with a 10.5-cm ID QFF for particulate phase. Compounds in the gas phase were collected in a modified cartridge (6 cm ID, 10 cm thickness) containing XAD-2 resin placed between layers of PUF.¹ Prior to sampling, all filters were cleaned by baking in a muffle furnace, while PUF plugs were cleaned by solvent extraction. Field blanks were prepared at the sites ($n = 5, 9,$ and $4,$ respectively) following the standard protocol for mounting QFF and PUF plugs without turning on the sampler. Košetice samples were analyzed for their organic carbon (OC) and elemental carbon (EC) contents using thermal-optical method with a Sunset Laboratory Model-4 semi-continuous field analyzer. At Grenoble, this was done following the EUSAAR-2 protocol using a Sunset Laboratory Dual-Optical Carbonaceous Analyzer, while the Urla samples were analyzed using a Magee Scientific SootScan OT21 Transmissometer.

Košetice samples were spiked with a surrogate solution containing d_8 -naphthalene, d_{10} -phenanthrene, and d_{12} -perylene, and extracted with dichloromethane using an automatic

extraction system (Büchi B-811). The extracts were concentrated under a gentle stream of nitrogen in ambient temperature and fractionated using a silica column. The mean surrogate recoveries were found to be 72 ± 14 , 88 ± 11 , and 102 ± 6 (mean \pm standard deviation), respectively. For Grenoble samples, QFF punches of 4.7-cm ID were extracted using a Dionex accelerated solvent extraction system (ASE 200) with dichloromethane, whereas PUF plugs were extracted using ASE 350 with acetone.² The PAH recoveries for the applied analytical method were checked using a certified reference material (NIST SRM 1649B), and the recoveries were within 80 – 120% of the certified values. The method performance for individual samples was checked using a surrogate standard, 6-methylchrysene, which was spiked onto the samples prior to extraction. The surrogate recovery was $91\pm 13\%$ across the samples. QFF samples from Urla were extracted using an ultrasonic bath, while PUF plugs were extracted using a Soxhlet extractor with 1:1 acetone:hexane.³ The extracts were cleaned and fractionated using an alumina-silicic acid column. Prior to extraction, all samples were spiked with a surrogate solution containing naphthalene-d₈, acenaphthene-d₁₀, phenanthrene-d₁₀, chrysene-d₁₂, and perylene-d₁₂; on average, the surrogate recoveries were 95 ± 9 , 101 ± 10 , 102 ± 19 , 93 ± 24 , and $85\pm 22\%$, respectively. Samples from Košetice and Urla were analyzed for PAHs using an Agilent gas chromatograph (GC 6890) interfaced to an Agilent mass selective detector (MS 5973) in electron impact mode, whereas samples from Grenoble were analyzed using a Thermo Scientific liquid chromatograph (UPLC Dionex Ultimate 3000) coupled with an ultraviolet/fluorescence detector. Analyte quantification for samples from Košetice and Grenoble was done using external calibration method, while that from Urla was performed following internal calibration procedure. Limits of quantification (LOQ) for analytes were calculated based on instrument detection limits, which in turn are determined using 3 times the chromatogram baseline noise level. LOQ values

were used in cases where analyte concentrations in blanks were <LOQ. Where individual PAH concentrations in samples exceeded the mean blank concentrations +3 standard deviations (SD), the mean blank concentrations (see Table S1) were subtracted from those in the corresponding samples. Overall, the analyte concentrations in blanks were <30% of those in samples. Data points for which the analyte concentrations were <LOQ in *both* gas and particulate phases were not considered for gas-particle partitioning calculations; however, in cases where the analyte concentrations were <LOQ only in *one of the two phases*, <LOQ was replaced with LOQ/2.

We estimated sample-specific/temperature-corrected breakthrough volumes for the target analytes using a ppLFER equation suggested by Kamprad and Goss⁴ for sorption of organic compounds to PUF. Sampling efficiency is expected to be >90% when the sampled air volume is less than *half the 50% breakthrough volume* (i.e. safe sampling volume). Subsequently, analyte concentrations for which the sampled air volume was larger than the estimated *safe sampling volume* were discarded (this was mainly needed for phenanthrene). The median estimated safe sample volumes are listed in Table S1.

Table S1 Estimated safe sampling volumes (m³) in the gas phase and analyte concentrations (mean ± standard deviation) in field blanks (G: gas phase; P: particulate phase)

	Safe Sampling volumes (m ³)			Blank concentrations (ng m ⁻³)		
	Median			Mean ± standard deviation		
	Košetice	Grenoble	Urla	Košetice	Grenoble	Urla
PHE	1.8×10 ³	1.0×10 ³	1.7×10 ²	G: 0.018±0.006 P: 0.005±0.0002	G: 0.157±0.069 P: 0.014±0.010	G: 0.670±0.212 P: 0.234±0.031
FLT	4.0×10 ⁴	2.0×10 ⁴	2.7×10 ³	G: 0.004±0.001 P: <LOQ	G: 0.026±0.015 P: 0.018±0.025	G: 0.059±0.015 P: 0.039±0.006
PYR	7.8×10 ⁴	3.9×10 ⁴	4.7×10 ³	G: 0.003±0.001 P: <LOQ	G: 0.015±0.007 P: 0.018±0.023	G: 0.051±0.014 P: 0.034±0.005
BAA	7.4×10 ⁵	3.5×10 ⁵	3.7×10 ⁴	G: <LOQ P: <LOQ	G: 0.035±0.024 P: 0.008±0.005	G: <LOQ P: 0.002±0.001
CHR	7.0×10 ⁵	3.3×10 ⁵	3.5×10 ⁴	G: <LOQ P: <LOQ	G: 0.003±0.002 P: 0.011±0.009	G: 0.007±0.001 P: 0.008±0.002
BBF	1.9×10 ⁷	8.1×10 ⁶	6.8×10 ⁵	G: <LOQ P: <LOQ	G: 0.002±0.001 P: 0.007±0.000	G: <LOQ P: <LOQ

Safe sampling volumes, defined as half the 50% breakthrough volumes, were estimated using a ppLFER equation developed for organic compound sorption to polyurethane, and corrected for the effect of ambient temperature during sampling interval using solute-specific enthalpies of phase transfer.⁴ The sampling efficiency would typically be ≥90% if the sampled air volume is less than half the 50% breakthrough volume.

S2 Junge-Pankow model

This model was originally suggested by Junge⁵ and later reviewed by Pankow⁶, and it assumes that SOCs are adsorbed onto the surface of PM. This model calculates θ using Eq. S1,

$$\theta = \frac{c_J S}{[c_J S + p_L^0]} \quad \text{Eq. S1}$$

The model relates θ to the analyte sub-cooled liquid vapor pressure, p_L^0 (Pa), particulate matter (PM) surface concentration, S (cm²_{surface} cm⁻³_{air}), and a constant, c_J (17.2 Pa cm for an unspecified sorbent). The latter depends on the analyte physico-chemical properties and ambient temperature. For individual analytes, c_J can be determined using measured θ and S , as well as temperature-corrected p_L^0 through Eq. S2,

$$c_j = \frac{\theta p_L^0}{s(1 - \theta)} \quad \text{Eq. S2}$$

Previous studies relied on constant values for S , except Lammel et al.⁷ and Landlová et al.⁸ where measured S was used. In the present study, we determined sample-specific S using PM number size distribution, assuming spherical particles. The p_L^0 values at 298 K were obtained from the literature⁹⁻¹¹ and corrected for changes in the average ambient temperature during each sampling event.

Experimental θ can be converted to K_P ($\text{m}^3_{\text{air}} \text{g}^{-1}_{\text{PM}}$) using Eq. S3,

$$K_P = \frac{\theta}{c_{\text{PM}}(1 - \theta)} \quad \text{Eq. S3}$$

where c_{PM} is PM concentration in air (g m^{-3}).

S3 Finizio and Dachs-Eisenreich models

An absorptive mechanism for partitioning of SOCs, based on their vapor pressure, was originally proposed by Pankow¹². This mechanism was later described in relation to the substance octanol-air partitioning coefficient, K_{OA} (unitless), by Finizio et al.¹³, and it assumes that SOCs partition into PM by diffusing through a viscous organic film that coats PM. For this model, K_P was calculated using Eq. S4,

$$K_P = 10^{-6} \left(\frac{f_{\text{OM}}}{\rho_{\text{OCT}}} \times \frac{\gamma_{\text{OCT}} M_{\text{OCT}}}{\gamma_{\text{OM}} M_{\text{OM}}} \right) K_{\text{OA}} \quad \text{Eq. S4}$$

where f_{om} (unitless) is the fraction of organic matter (OM) in PM, ρ_{OCT} (0.82 kg L^{-1}) is the density of octanol, γ_{OCT} and γ_{OM} (unitless) are activity coefficients of the target compound in octanol and organic matter, respectively, M_{OCT} and M_{OM} are molecular mass of octanol (130 g mol^{-1}) and organic matter, respectively. Assuming that octanol imitates organic matter in PM,

Harner and Bidleman¹⁴ suggested that the ratio of $\gamma_{\text{OCT}}/\gamma_{\text{OM}}$ and $M_{\text{OCT}}/M_{\text{OM}}$ can be assumed to be 1. For model calculations, experimentally determined K_{OA} values were obtained from Harner and Bidleman¹⁵ and Odabasi et al.¹¹ and corrected for changes in ambient temperature in each sampling event.

Previous studies noted that the model of Finizio underestimated K_{P} for PAHs.^{11, 14, 16} This was suggested to be due to underestimation of the term $\gamma_{\text{OCT}}/\gamma_{\text{OM}}$ or possibly due to the high affinity of PAHs to soot particles, a parameter that is not accounted for in that model. Dachs and Eisenreich¹⁶ suggested the use of a dual-model that, in addition to absorption into organic matter, accounts for adsorption onto soot particles. This model can be formulated as Eq. S5,

$$K_{\text{P}} = 10^{-6} \left[\left(\frac{f_{\text{OM}}}{\rho_{\text{OCT}}} \times \frac{\gamma_{\text{OCT}} M_{\text{OCT}}}{\gamma_{\text{OM}} M_{\text{OM}}} \right) K_{\text{OA}} + \left(f_{\text{EC}} \times \frac{a_{\text{EC}}}{a_{\text{soot}}} \right) K_{\text{SA}} \right] \quad \text{Eq. S5}$$

where f_{EC} (unitless) is the fraction of elemental carbon (EC) in PM, a_{EC} and a_{soot} ($\text{m}^2 \text{g}^{-1}$) are specific surface area of EC and soot, respectively, and K_{SA} (L kg^{-1}) is soot-air partitioning coefficient. The latter was calculated using a thermodynamic estimation model suggested by van Noort¹⁷, Eq. S6

$$\log K_{\text{SA}} = -0.85 \log p_{\text{L}}^0 + 8.94 - \log (998/a_{\text{soot}}) \quad \text{Eq. S6}$$

The value of $18.21 \text{ m}^2 \text{g}^{-1}$ was used for a_{soot} in the present study; this was the geometric mean of surface areas reported by Jonker and Koelmans¹⁸ for traffic, wood, coal, and diesel soot samples (i.e. 59.4, 3.6, 8.2, and $62.7 \text{ m}^2 \text{g}^{-1}$).

S4 Methodology for ppLFER calculations

K_p was calculated using Abraham solute descriptors from Table S2 and ppLFER models from Table S3, by summing the individual partitioning coefficients from adsorption and absorption processes related to inorganic and organic PM components, Eq. S7,

$$K_p (\text{m}_{\text{air}}^3 \text{g}_{\text{PM}}^{-1}) = [(K_{\text{EC}} \times a_{\text{EC}} \times f_{\text{EC}} + K_{(\text{NH}_4)_2\text{SO}_4} \times a_{(\text{NH}_4)_2\text{SO}_4} \times f_{(\text{NH}_4)_2\text{SO}_4} + K_{\text{NH}_4\text{Cl}} \times a_{\text{NH}_4\text{Cl}} \times f_{\text{NH}_4\text{Cl}}) + (K_{\text{DMSO}/\rho_{\text{DMSO}}} \times f_{\text{OM,A}} + K_{\text{PU}} \times f_{\text{OM,B}})] \quad \text{Eq. S7}$$

where K_{EC} , $K_{(\text{NH}_4)_2\text{SO}_4}$, and $K_{\text{NH}_4\text{Cl}}$ are the target substance partitioning (adsorption) coefficients ($\text{mol m}_{\text{surface}}^{-2}/\text{mol m}_{\text{air}}^{-3}$) for elemental carbon/diesel soot, ammonium sulfate, and ammonium chloride (the last two represent secondary inorganic aerosols), respectively, a_{EC} , $a_{(\text{NH}_4)_2\text{SO}_4}$, and $a_{\text{NH}_4\text{Cl}}$ are the adsorbent specific surface areas ($\text{m}_{\text{surface}}^2 \text{g}_{\text{adsorbent}}^{-1}$), and f_{EC} , $f_{(\text{NH}_4)_2\text{SO}_4}$, and $f_{\text{NH}_4\text{Cl}}$ are their mass fractions in PM ($\text{g}_{\text{adsorbent}} \text{g}_{\text{PM}}^{-1}$). The related fractions were determined using the concentrations of elemental carbon, SO_4^{2-} , and Cl^- measured in PM, taking into account the molar mass of $(\text{NH}_4)_2\text{SO}_4$ and NH_4Cl . This was subject to availability of the supporting information for each site – i.e. Cl^- concentrations were only available for Grenoble and PM inorganic constituents were not measured at Urla. In addition, OC and EC concentrations in PM were measured once every six days at Košetice. Consequently, only 46 samples could be considered for model calculations at this site (this applies to Finizio and Dachs-Eisenreich models as well). We were not able to include ammonium nitrate in our model calculations due to the lack of relevant ppLFER system parameters. Furthermore, we excluded adsorption to NaCl because that is a typical constituent of marine inorganic aerosols and it was not considered relevant for samples from Grenoble and Košetice. In addition, for samples from Urla, we were not able to calculate NaCl fraction in PM due to the lack of Cl^- measurements. Nevertheless,

considering NaCl and NH₄Cl system parameters in Table S3 (specific surface area 0.10 and 0.08 m² g⁻¹, respectively; molar mass: 58.44 and 53.49 g mol⁻¹, respectively), the contribution of adsorption onto NaCl would be smaller than that for NH₄Cl (i.e. log K_P PYR at 288 K and 60% RH: -0.68 and -0.13 m³_{air} g⁻¹_{adsorbent}, respectively). Hence, similar to that for NH₄Cl, PAH adsorption to NaCl can be neglected when studying gas-particle partitioning (see section 4.2 in the text). For a_{EC} , the geometric mean of 18.21 m² g⁻¹ was calculated from the values reported for traffic, wood, coal, and diesel soot,¹⁸ whereas, $a_{(NH_4)_2SO_4}$, and a_{NH_4Cl} were taken from another study.¹⁹

K_{DMSO} (m³_{air} m⁻³_{DMSO}) and K_{PU} (m³_{air} g⁻¹_{PU}) are the substance partitioning (absorption) coefficients for dimethyl sulfoxide-air and polyurethane-air systems; ρ_{DMSO} is dimethyl sulfoxide density (g m⁻³); $f_{OM,A}$ and $f_{OM,B}$, are mass fractions of absorbing phases (g_{adsorbent} g⁻¹_{PM}), corresponding to (A) low to high molecular mass both water soluble (WS) and organic soluble (OS) organic matter (OM) and (B) high molecular mass organic polymers (OP).

S5 Information on chemistry of organic phases considered for ppLFER model

HULIS have been found in high quantities in the water soluble fraction of PM, and partly in the water insoluble fraction.²⁰ They were initially thought to be made of organic polymers; however, it was shown later that they are most likely made of weak, partly aromatic polyacids,²¹ with molecular mass in the range of 200 to 500 Da.²² More precisely, Kiss et al.²³ noted that the water soluble fraction of PM, with which HULIS is associated, may contain polyconjugated aromatic or aliphatic structures, including short-chain carboxylic acids, hydroxyl acids, and polyhydroxy substances.

The presence of polymers in PM has been previously noted.²⁴⁻²⁶ Their potential effect on gas-particle partitioning of SOCs was suggested by Roth et al.²⁷ In that study, increasing the relative humidity to 80% resulted in higher sorption capacity of the studied PM, which was attributed to the conversion of glassy polymers to semi-solid form. Organic polymers could originate from natural sources (e.g. cellulose) as well as condensation and polymerization of gaseous organics in the atmosphere. Puxbaum and Tenze-Kunit²⁵ noted that about 16% of the PM insoluble organic matter from downtown Vienna was made of cellulose. Moreover, chamber experiments showed that up to 50% of the secondary organic aerosols, which in turn can form up to 90% of the urban PM organic mass,²⁸ could be made of polymers with 400 to 900 Da mass range,²⁴ following polymerization of carbonyls and their hydrates in the atmosphere.

While the existence of hydrophilic and hydrophobic OM fractions has been recognized since decades,²⁹⁻³¹ due to methodological limitations, the knowledge of chemical composition of OM mass is still largely deficient. Only ~ 3-5% of OM could be attributed to substance groups,^{32, 33} while the rest is not extractable/elutable or cannot be resolved on chromatographic columns. Furthermore, even identical chemical compositions could lead to differences in gas-particle partitioning due to inhomogeneous mixing on the individual particle level (e.g. shell-like structure) or due to different phase state.³⁴

Regarding the water insoluble organic matter (e.g. aliphatic organics) in PM, and the estimation/allocation of organic sub-fractions for ppLFER analysis following Rogge et al.³² study, it should be noted that the resolved organic fraction from Rubidoux contained ~5% *n*-alkanes, but higher quantities could be expected for samples from the central European sites, presumably due to higher influence of primary and secondary biogenic sources of OM. Oliveira

et al.³⁵ found between 11 and 16% *n*-alkanes in the resolved fraction of PM collected from continental sites in central and Western Europe.

Table S2 Abraham solute descriptors used for ppLFER calculations

	<i>E</i>	<i>S</i>	<i>A</i>	<i>B</i>	<i>V</i>	<i>L</i>	Reference
PHE	1.92	1.28	0.00	0.29	1.45	7.71	Ariyasena and Poole ³⁶
FLT	2.38	1.55	0.00	0.24	1.59	8.83	Sprunger et al. ³⁷
PYR	2.81	1.71	0.00	0.28	1.59	8.83	Sprunger et al. ³⁷
BAA	2.74	1.68	0.00	0.37	1.82	10.12	Ariyasena and Poole ³⁶
CHR	2.59	1.66	0.00	0.29	1.82	10.14	Ariyasena and Poole ³⁶
BBF	3.19	1.82	0.00	0.40	1.95	11.63	Abraham et al. ³⁸

Table S3 ppLFER system parameters

System	Unit	<i>e</i>	<i>s</i>	<i>a</i>	<i>b</i>	<i>v</i>	<i>l</i>	<i>c</i>	T(K)	Reference
Dry octanol-air	$L_{\text{air}} L_{\text{solvent}}^{-1}$	-0.21	0.56	3.51	0.75	-	0.94	-0.22	298	Abraham et al. ³⁹
Dry N,N-dimethylformamide	$L_{\text{air}} L_{\text{solvent}}^{-1}$	-0.87	2.11	3.77	0.00	-	1.01	-0.39	298	Abraham et al. ³⁹
Dry dimethyl sulfoxide-air	$L_{\text{air}} L_{\text{solvent}}^{-1}$	-0.22	2.90	5.04	0.00	-	0.72	-0.56	298	Abraham et al. ³⁹
Dry acetone-air	$L_{\text{air}} L_{\text{solvent}}^{-1}$	-0.39	1.73	3.06	-	-	0.87	0.13	298	Abraham et al. ⁴⁰
Aerosol, Berlin winter	$m_{\text{air}}^3 g_{\text{aerosol}}^{-1}$	-	1.38	3.21	0.42	0.98	0.63	-7.24	288	Arp et al. ⁴¹
Aerosol, Dübendorf autumn	$m_{\text{air}}^3 g_{\text{aerosol}}^{-1}$	-	1.19	3.37	0.03	0.73	0.66	-7.08	288	Arp et al. ⁴¹
Polyurethane ether (PU)-air	$L_{\text{air}} \text{kg}_{\text{PU}}^{-1}$	-	1.69	3.66	0.00	0.36	0.71	-0.15	288	Kamprad and Goss ⁴
NIST diesel soot-air	$m_{\text{air}}^3 m_{\text{surface}}^{-2}$	-	-	2.70	2.45	-	1.09	-8.47	288	Roth et al. ⁴²
(NH ₄) ₂ SO ₄ (60% RH)	$m_{\text{air}}^3 m_{\text{surface}}^{-2}$	-	-	2.13	5.34	-	0.88	-8.47	288	Goss et al. ¹⁹
NH ₄ Cl (60% RH)	$m_{\text{air}}^3 m_{\text{surface}}^{-2}$	-	-	2.28	4.72	-	0.92	-8.47	288	Goss et al. ¹⁹
NaCl (60% RH)	$m_{\text{air}}^3 m_{\text{surface}}^{-2}$	-	-	2.86	4.82	-	0.84	-8.47	288	Goss et al. ¹⁹

Table S4 Minimum, maximum, and median PAH particulate mass fractions (Θ ; unitless), ambient temperature (T; °C), and PM sample compositions

	Košetice ($n = 150$) ^a			Grenoble ($n = 114$) ^b			Urla ($n = 18$)		
	Min.	Max.	Med.	Min.	Max.	Med.	Min.	Max.	Med.
PHE	0.00	0.53	0.03	0.01	0.54	0.02	NA	NA	NA
FLT	0.00	0.92	0.24	0.04	0.93	0.11	0.00	0.28	0.07
PYR	0.01	0.96	0.36	0.04	0.96	0.15	0.00	0.35	0.10
BAA	0.05	1.00	0.96	0.43	1.00	0.78	0.33	0.83	0.64
CHR	0.08	1.00	0.80	0.02	1.00	0.54	0.19	0.78	0.40
BBF	0.69	1.00	0.99	0.67	1.00	0.98	0.68	0.97	0.90
T	-13.2	25.8	8.4	-1.9	30.2	13.9	22.8	33.1	27.8
PM₁₀	5.0	96.1	16.5	2.0	75.0	21.5	24.8	75.8	44.3
f_{OM}	0.10	0.84	0.39	0.13	0.83	0.37	0.19	0.58	0.32
f_{EC}	0.00	0.05	0.02	0.02	0.19	0.06	0.01	0.04	0.03
$f_{(\text{NH}_4)_2\text{SO}_4}$	0.05	0.39	0.17	0.02	0.71	0.11	NA	NA	NA
$f_{\text{NH}_4\text{Cl}}$	NA	NA	NA	0.000	0.105	0.004	NA	NA	NA
f_{HULIS}	NA	NA	NA	0.04	0.36	0.14	NA	NA	NA
f_{WSOM}	NA	NA	NA	0.21	0.65	0.47	NA	NA	NA

^a the source of the data is Shahpoury et al.⁴³; ^b the source of the data is Tomaz et al.⁴⁴; Particulate matter concentrations (PM₁₀; $\mu\text{g m}^{-3}$), fractions of organic matter (f_{OM} ; unitless), elemental carbon (f_{EC} ; unitless), ammonium sulfate ($f_{(\text{NH}_4)_2\text{SO}_4}$; unitless), and ammonium chloride ($f_{\text{NH}_4\text{Cl}}$; unitless) in PM; the fraction of humic-like substances (f_{HULIS} ; unitless), and water soluble organic matter (f_{WSOM} ; unitless) in OM; NA: not available; $n = 46$ for f_{OM} and f_{EC} at Košetice.

Figure S1A PAH particulate mass fractions (Θ) as a function of temperature at Košetice. Data points which were subject to breakthrough were excluded; this only applied to PHE.

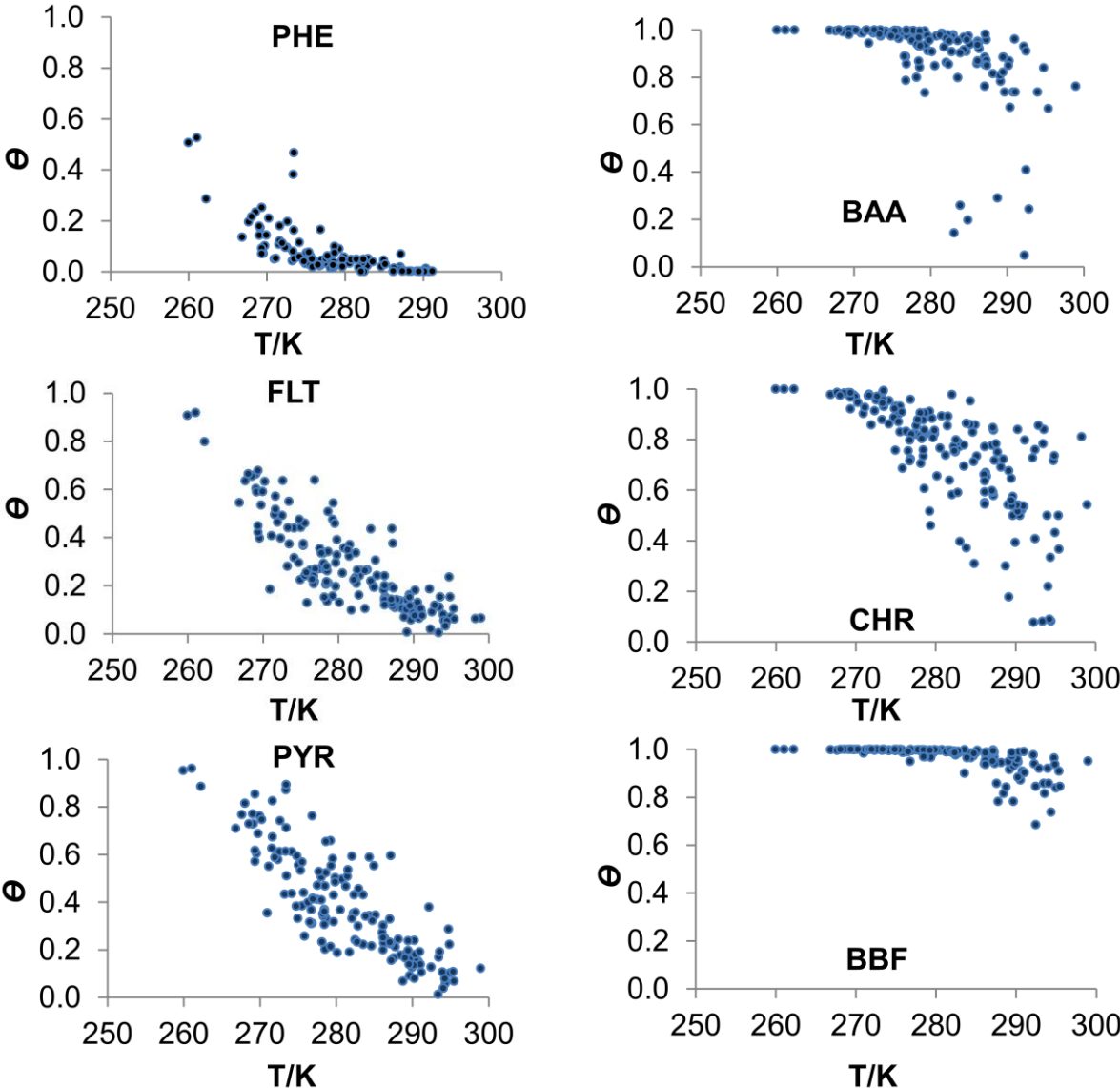


Figure S1B PAH particulate mass fractions (Θ) as a function of temperature at Grenoble. Data points which were subject to breakthrough were excluded; this only applied to PHE.

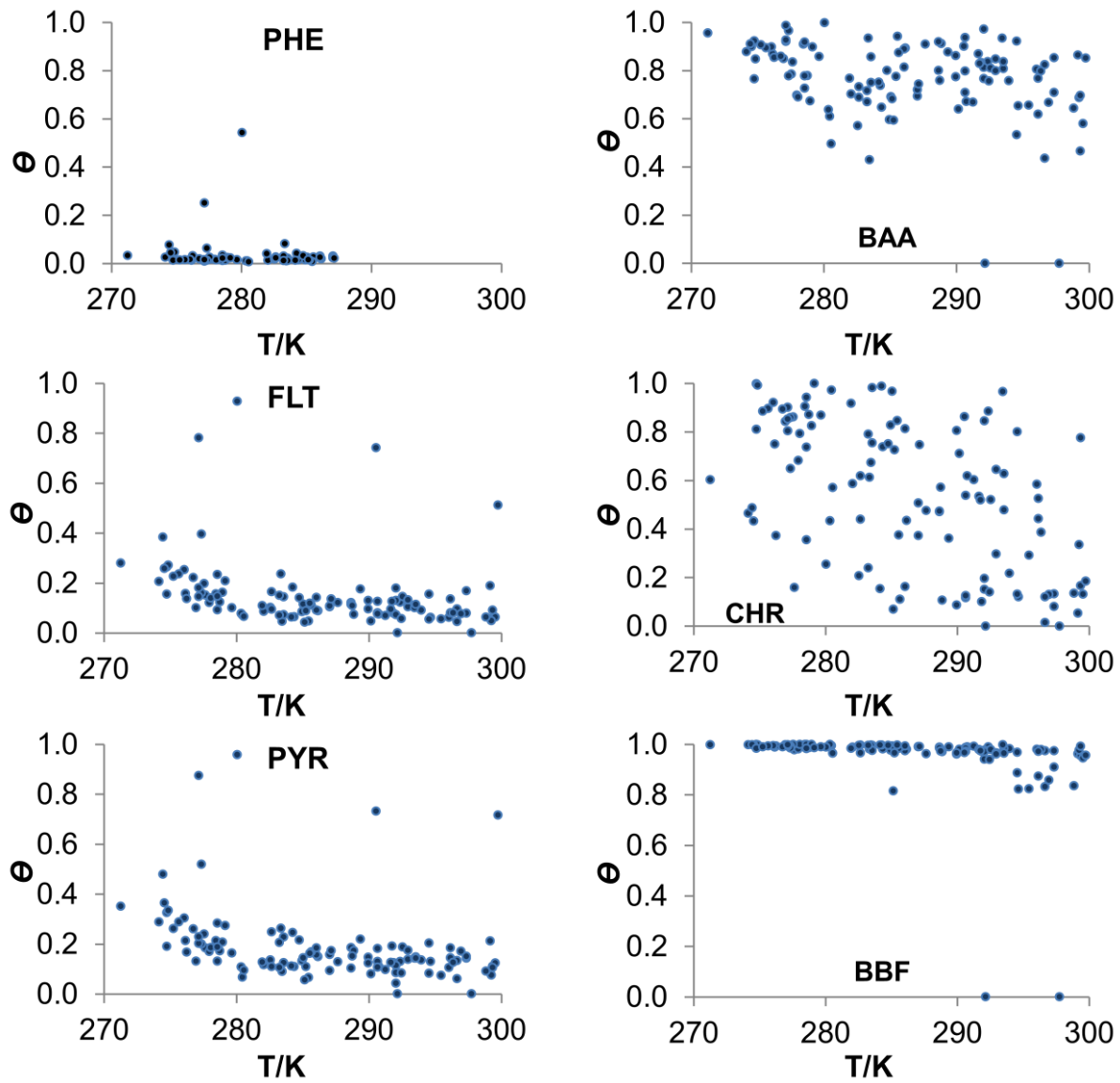
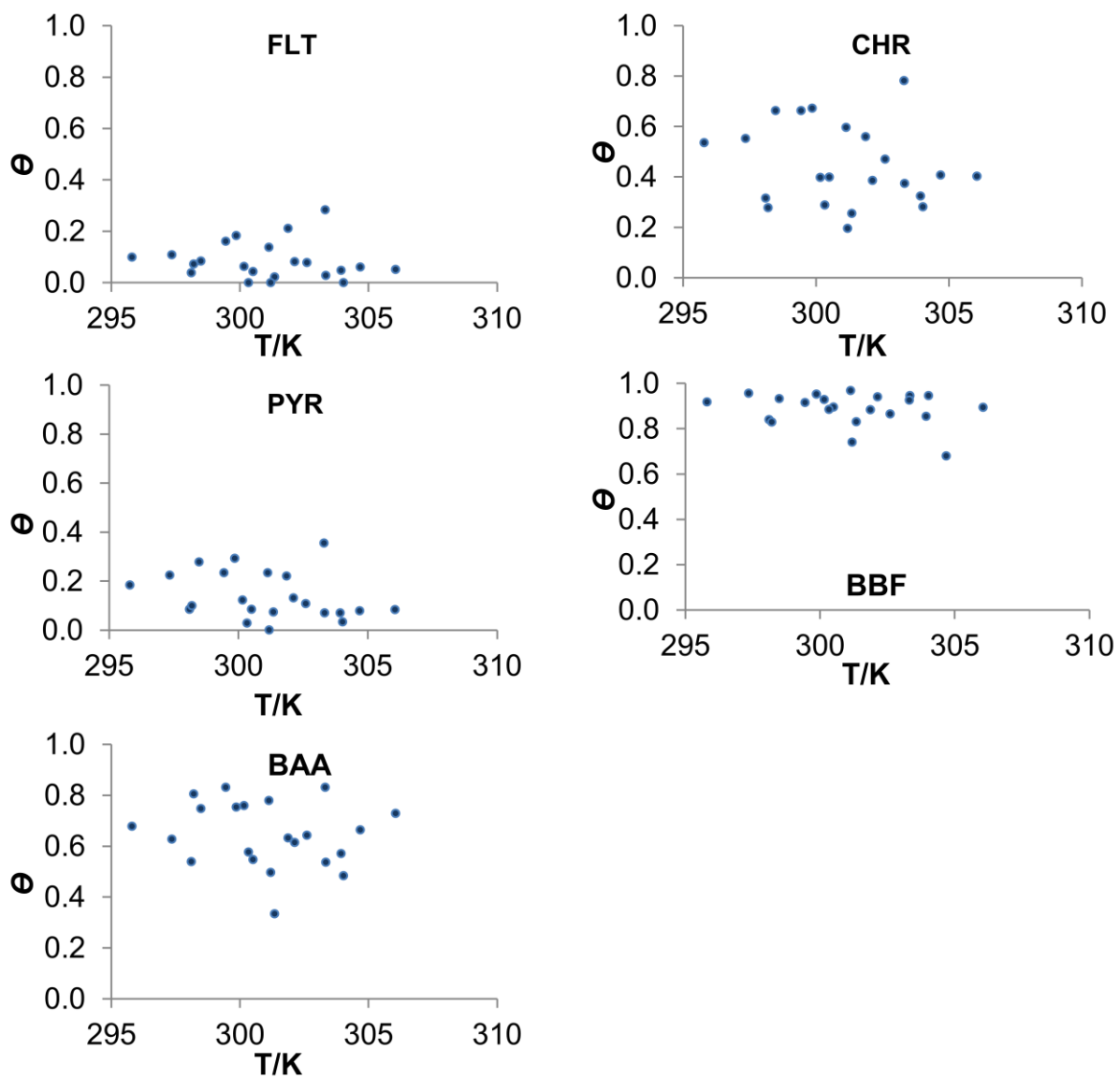


Figure S1C PAH particulate mass fractions (Θ) as a function of temperature at Urla; PHE was excluded due to analytical uncertainties



S6 Model predictions

S6.1 ppLFER model predictions

Figure S2 Predicted versus experimental $\log K_P$ ($\text{m}^3_{\text{air}} \text{g}^{-1} \text{PM}$) for Košetice ($n = 56$), ppLFER model based on organic aerosol from Dübendorf autumn (A) and Berlin winter (B) (see Table S3). The predicted K_P values were corrected for the effect of ambient temperature using enthalpy of vaporization for each compound. RMSE for (A): PHE: 2.33, FLT: 2.25, PYR: 2.44, BAA: 2.77, CHR: 2.12, BBF: 2.14. RMSE for (B): PHE: 2.01, FLT: 1.90, PYR: 2.04, BAA: 2.33, CHR: 1.71, BBF: 1.69.

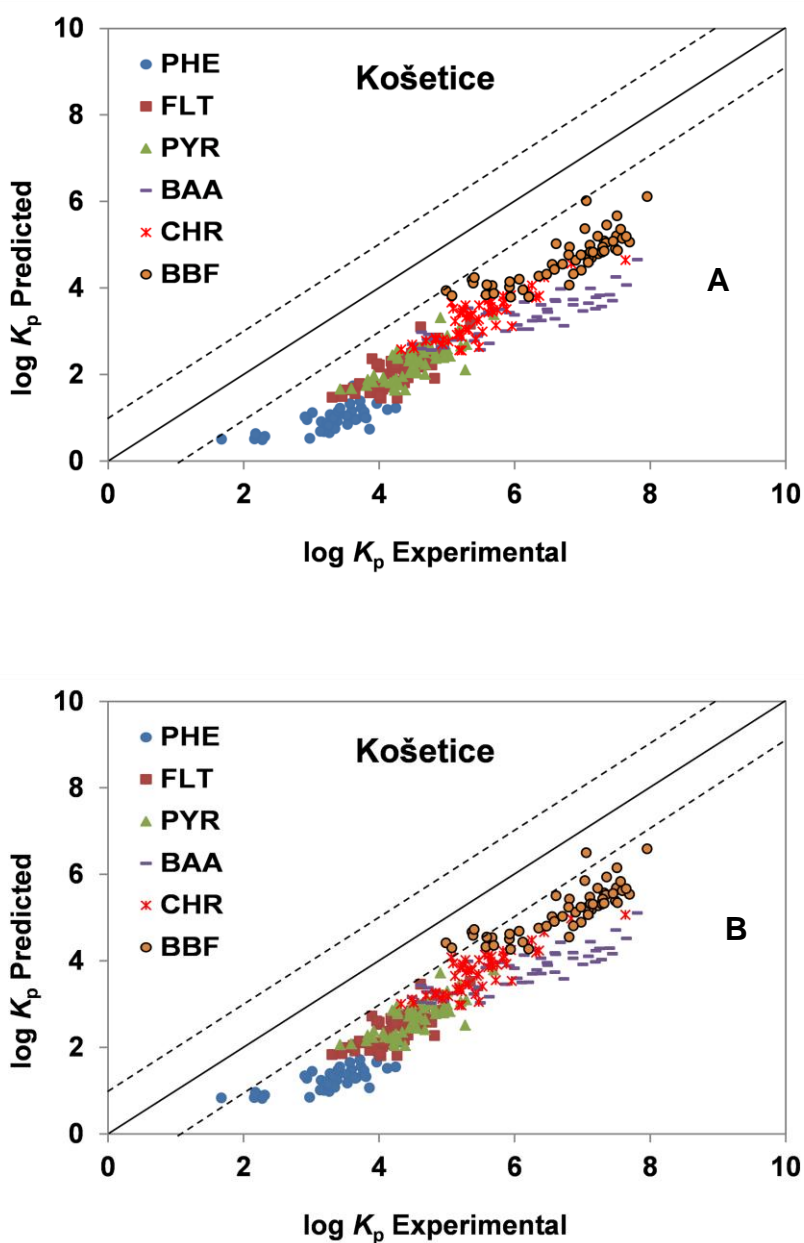


Figure S3 Predicted versus experimental $\log K_P$ ($\text{m}^3_{\text{air}} \text{g}^{-1}_{\text{PM}}$) for Grenoble ($n = 114$), multi-phase ppLFFER model using measured f_{WSOM} (Phase A) and $1 - f_{\text{WSOM}}$ (Phase B)

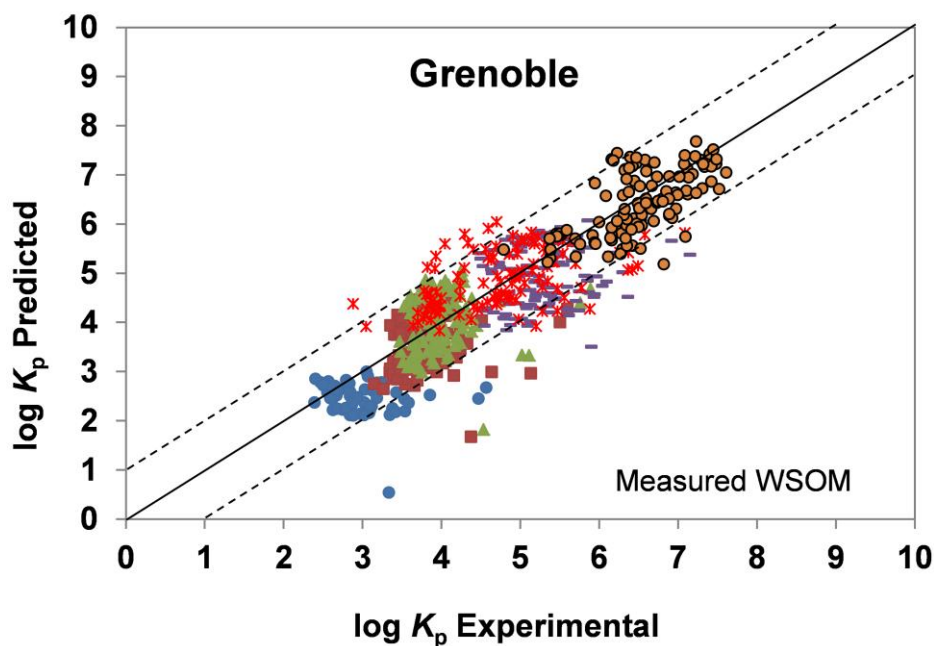


Table S5 Root mean square errors and percentage of data points predicted within one order of magnitude accuracy (in parenthesis) for Grenoble dataset using a range of soot specific surface areas (i.e. 3.60, 18.21, and 62.70 $\text{m}^2 \text{g}^{-1}$)

	Dachs-Eisenreich Model			ppLFFER		
	<i>3.60</i>	<i>18.21</i>	<i>62.70</i>	<i>3.60</i>	<i>18.21</i>	<i>62.70</i>
PHE	1.02 (63)	0.92 (69)	0.75 (83)	0.69 (85)	0.68 (85)	0.66 (86)
FLT	1.01 (57)	0.94 (67)	0.80 (82)	0.56 (96)	0.56 (96)	0.56 (96)
PYR	1.11 (48)	1.02 (57)	0.85 (75)	0.59 (92)	0.59 (91)	0.59 (91)
BAA	0.96 (63)	0.93 (65)	0.84 (73)	0.72 (84)	0.72 (84)	0.70 (84)
CHR	0.70 (84)	0.68 (84)	0.66 (83)	0.71 (83)	0.72 (83)	0.72 (83)
BBF	0.95 (60)	0.90 (68)	0.80 (82)	0.50 (95)	0.49 (96)	0.49 (94)

ppLFFER: poly-parameter linear free energy relationship; specific surface area of 18.21 $\text{m}^2 \text{g}^{-1}$ is the geometric mean of 3.6 (wood soot), 8.2 (coal soot), 59.4 (traffic soot), and 62.7 (diesel soot) taken from Jonker and Koelmans¹⁸. Regardless of the selected surface area, the predictions made with the ppLFFER model were superior to those with Dachs-Eisenreich model, with the exception of CHR for which the models returned comparable results.

161 **S6.2 Multiphase ppLFER model predictions with substances other than PAHs**

162 We tested the multi-phase ppLFER model for four polychlorinated dibenzofurans (PCDFs) from
163 50 gas-phase and PM samples collected in Košetice between December 2011 and December
164 2013, as well as eight nitro- and oxy-PAHs in samples from Grenoble collected between January
165 and December 2013. The calculations for both datasets were performed using estimated
166 Abraham solute descriptors from ACD/Absolv program,⁴⁵ and the latter dataset is the subject of
167 a companion paper.⁴⁴ Figure S4 shows the predictions made for furans; the model predicted the
168 partitioning constants for 2,3,7,8-tetrachlorodibenzofuran, 1,2,3,7,8-pentachlorodibenzofuran,
169 2,3,4,7,8- pentachlorodibenzofuran, and 1,2,3,4,7,8- hexachlorodibenzofuran reasonably well
170 with RMSE of $\log K_P$ ranging from 0.30 to 0.66. As also noted by Tomaz et al.⁴⁴, for oxy- and
171 nitro-PAHs, acenaphthenequinone, 9,10-anthraquinone, 9-phenanthrenecarboxaldehyde, 9-
172 nitroanthracene, and 9-nitrophenanthrene the model had made reasonably good predictions with
173 RMSE values ranging from 0.33 to 0.67, while the predictions for 3-nitrophenanthrene, 5-
174 nitroacenaphthene, and 6H-dibenzo[b,d]pyran-6-one were less accurate (RMSE: 0.82, 0.94, and
175 1.13, respectively).⁴⁴

176 In addition to the abovementioned substance classes, the ppLFER model was tested on 16 mono-
177 aromatic compounds (i.e. methyl benzoate, benzyl alcohol, buthyl benzene, pentyl benzene,
178 hexyl benzene, 1,2,4-trimethylbenzene, 1,3,5,- trimethylbenzene, 1,2-dichlorobenzene, 1,3-
179 dichlorobenzene, 1,4-dichlorobenzene, 1,2,4-trichlorobenzene, 1,4-dibromobenzene, 2 methyl
180 pyrazine, acetophenone, aniline, 2,6 dimethyl aniline) for which gas-particle partitioning
181 constants were reported by Arp et al.⁴¹. As can be seen from Figure S5, the model predicted the
182 observed K_P from Dübendorf autumn and Berlin winter samples within one order of magnitude
183 accuracy with RMSE of 0.62 and 0.52 log unit. Although the model showed some tendency to

184 overestimate the K_p for Dübendorf and Berlin data, we found similar performance when we
185 applied the Finizio model to these datasets (RMSE: 0.61 and 0.49) (Figure S5). It is not clear to
186 us why both models showed such behavior for this dataset. The ppLFER model presented here
187 has to be tested for more classes of environmentally relevant organic chemicals; however, we
188 believe that it performs reasonably well for the non-ionic mono- and poly-aromatic compounds
189 discussed here, particularly when experimentally determined Abraham solute descriptors are
190 used.

Figure S4 Predicted versus experimental $\log K_P$ ($\text{m}^3_{\text{air}} \text{g}^{-1}_{\text{PM}}$) for furans at Košetice ($n = 50$), multi-phase ppLFER model. RMSE for 2,3,7,8-TCDF: 0.30, 1,2,3,7,8-PeCDF: 0.49, 2,3,4,7,8-PeCDF: 0.39, 1,2,3,4,7,8-HxCDF: 0.66.

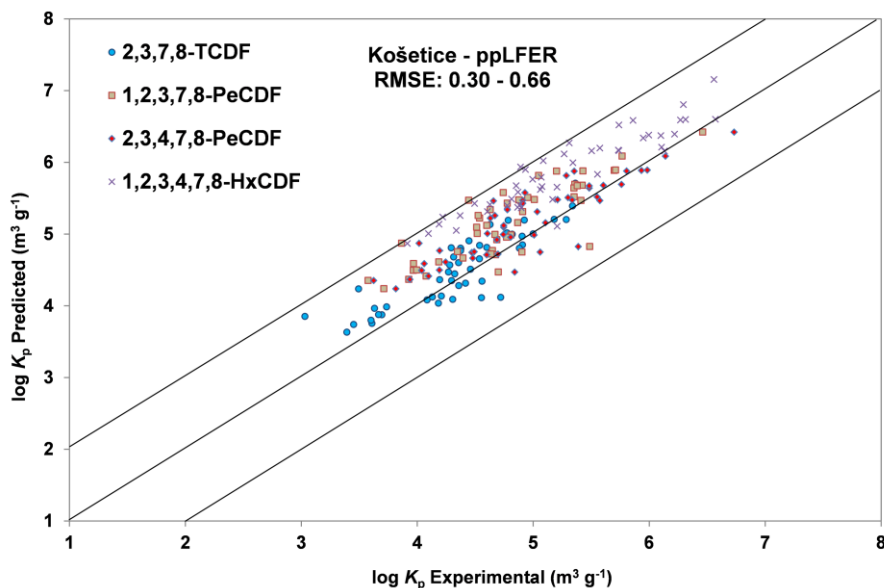
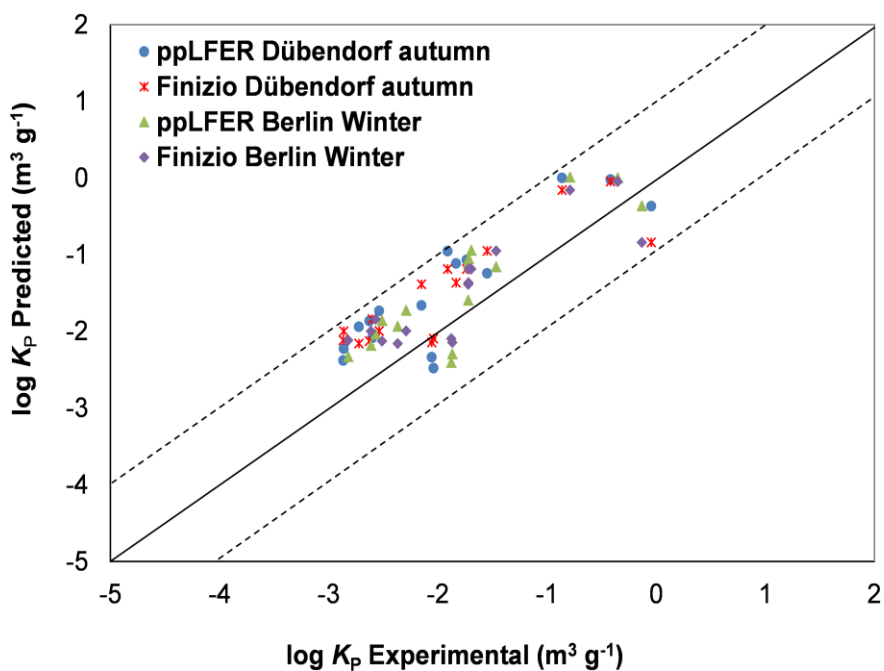


Figure S5 Partitioning constants ($\text{m}^3_{\text{air}} \text{g}^{-1}_{\text{PM}}$) predicted using multi-phase ppLFER and Finizio models versus observed values for 16 mono-aromatic compounds from Dübendorf autumn and Berlin winter samples reported by Arp et al.⁴¹



S6.3 spLFER model predictions

Figure S6 Median c_j (Pa cm) calculated using experimental θ , S , and p_L^0 (T) at Košetice

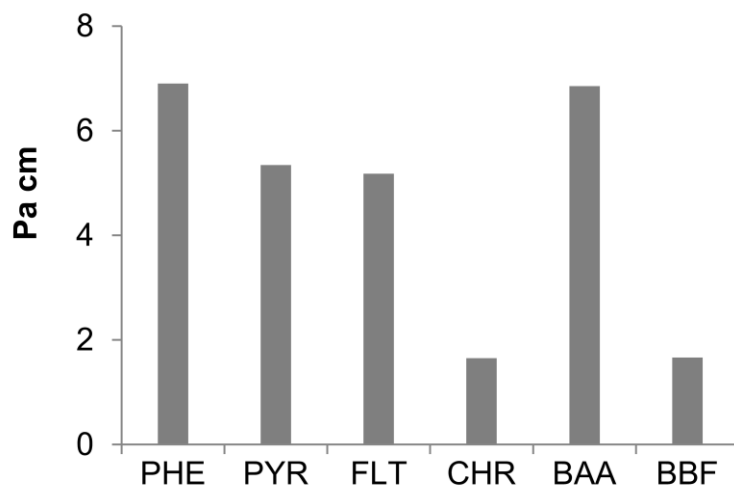


Figure S7 Median PM surface concentrations ($\text{cm}^2_{\text{surface}} \text{cm}^{-3}_{\text{air}}$) determined using PM number size distribution at Košetice

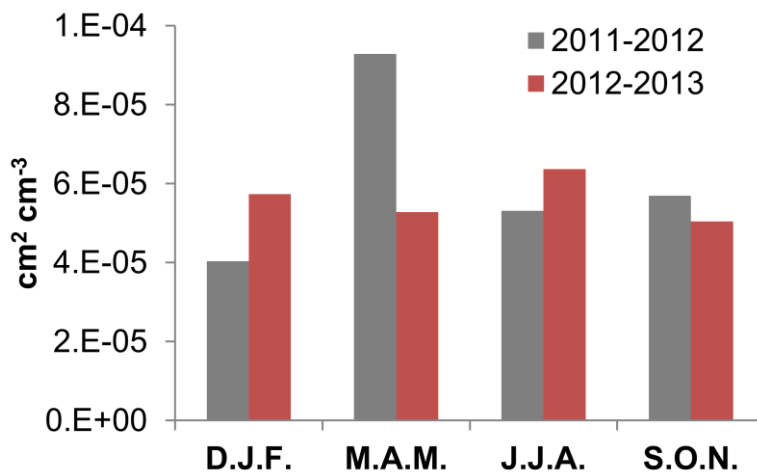


Table S6 Experimental c_j for individual PAHs

	Min.	Max.	Median	Mean	SD
PHE	0.25	56.15	6.90	9.50	9.14
FLT	0.12	20.11	5.18	4.49	3.96
PYR	0.13	624.59	5.34	5.19	74.77
BAA	0.06	155.42	6.85	6.02	21.74
CHR	0.03	15.80	1.65	1.44	2.25
BBF	0.02	15.62	1.66	1.30	2.61
BKF	0.02	5.50	0.58	0.53	1.00
BAP	0.01	5.46	0.44	0.38	0.91
IPY	0.00	1.71	0.11	0.07	0.26
BPE	0.00	0.30	0.05	0.04	0.06
DHA	0.00	0.02	0.00	0.00	0.00

c_j determined using experimental Θ , PM surface concentrations (S , see Fig. S7), and sub-cooled liquid vapor pressure, p_L^0 (T); phenanthrene (PHE), fluoranthene (FLT), pyrene (PYR), benzo(*a*)anthracene (BAA), chrysene (CHR), benzo(*b*)fluoranthene (BBF), benzo(*k*)fluoranthene (BKF), benzo(*a*)pyrene (BAP), indeno(1,2,3-120 *cd*)pyrene (IPY), benzo(*g,h,i*)perylene (BPE), dibenz(*a,h*)anthracene (DHA).

Figure S8 Predicted versus experimental $\log K_p$ ($\text{m}^3_{\text{air}} \text{g}^{-1}_{\text{PM}}$) for Košetice ($n = 150$), Junge-Pankow model

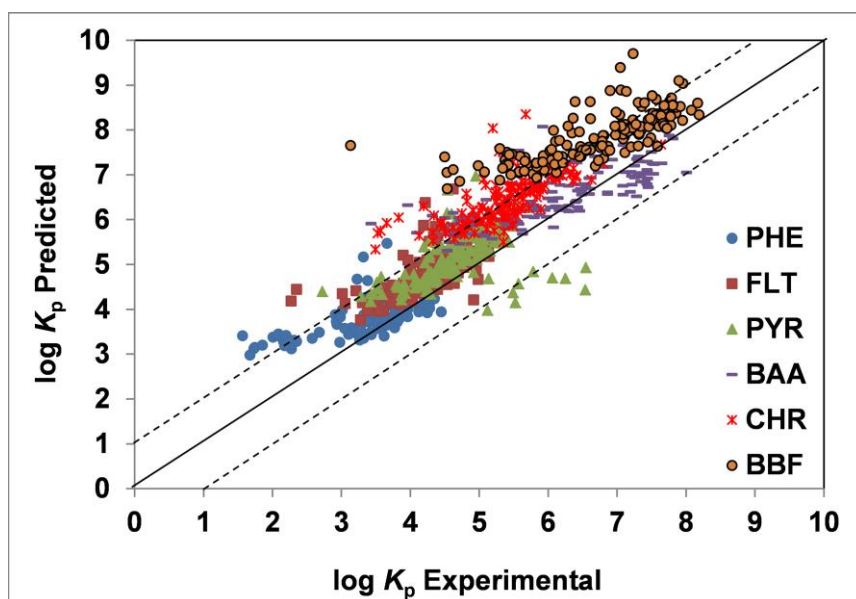


Figure S9 Predicted versus experimental $\log K_p$ ($\text{m}^3_{\text{air}} \text{g}^{-1}_{\text{PM}}$), Finizio and Dachs-Eisenreich models; $n = 46, 114,$ and 18 for Košetice, Grenoble, and Urla, respectively

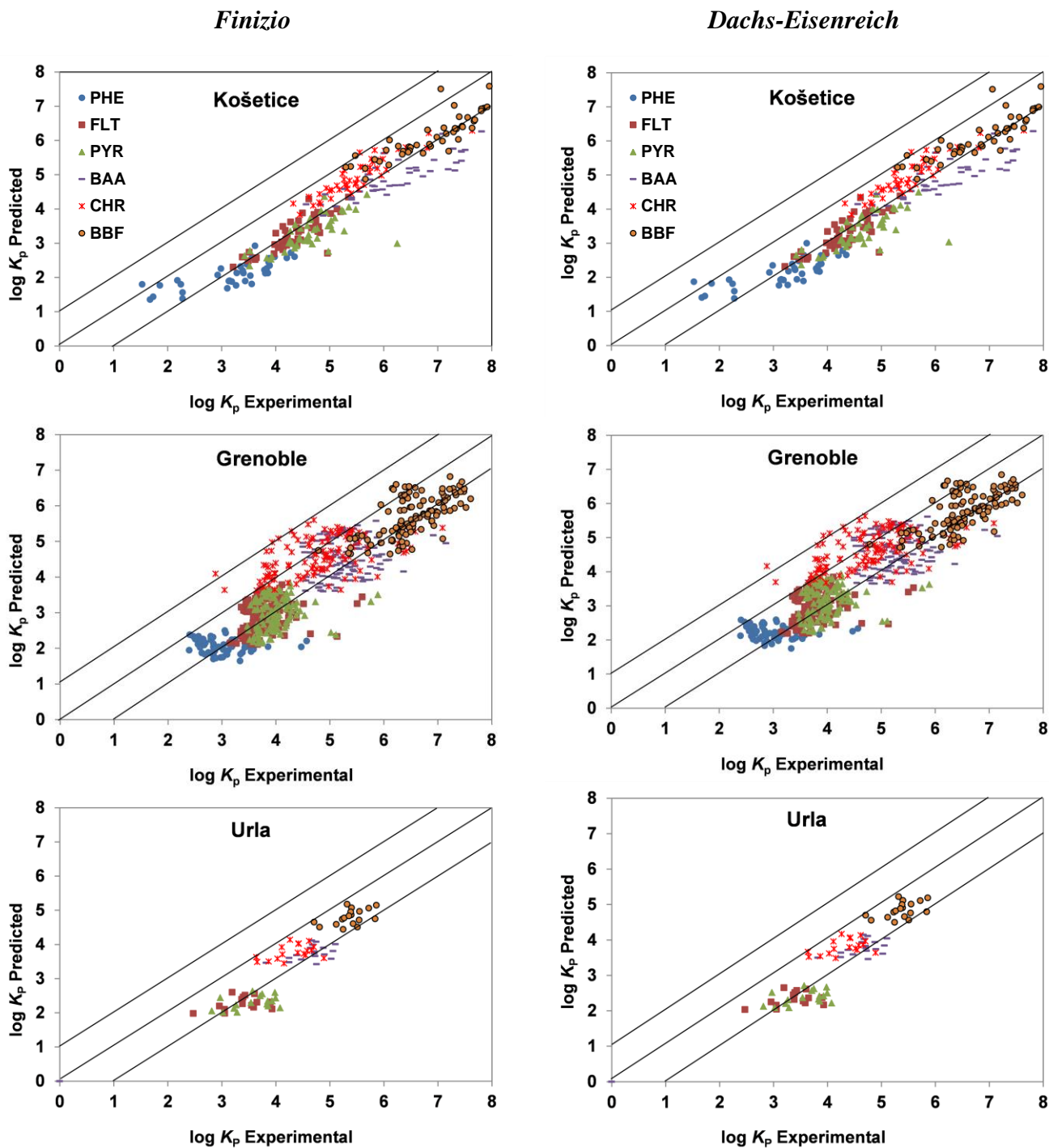
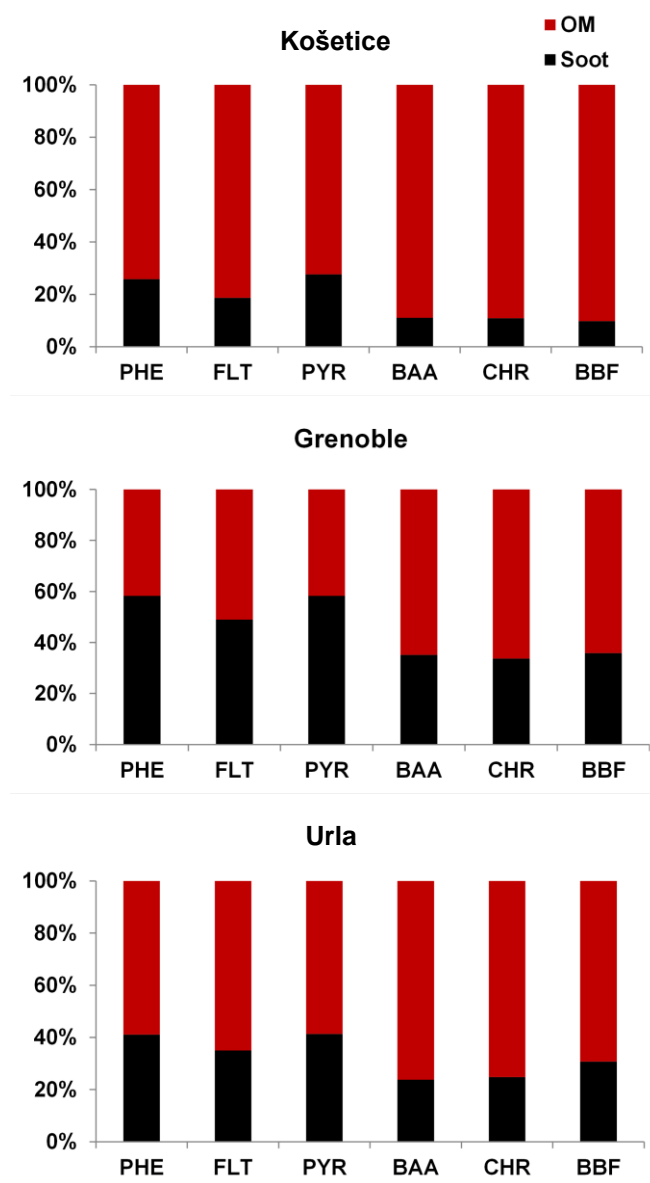


Figure S10 Median contributions of absorption into organic matter and adsorption onto soot for Dachs-Eisenreich model



References

1. Demircioglu, E.; Sofuoglu, A.; Odabasi, M. Atmospheric concentrations and phase partitioning of polycyclic aromatic hydrocarbons in Izmir, Turkey. *CLEAN – Soil, Air, Water* **2011**, *39* (4), 319-327.
2. Albinet, A.; Leoz-Garziandia, E.; Budzinski, H.; Villenave, E. Polycyclic aromatic hydrocarbons (PAHs), nitrated PAHs and oxygenated PAHs in ambient air of the Marseilles area (South of France): concentrations and sources. *Sci. Total Environ.* **2007**, *384* (1–3), 280-292.
3. Odabasi, M.; Cetin, B.; Bayram, A. Persistent organic pollutants (POPs) on fine and coarse atmospheric particles measured at two (urban and industrial) sites. *Aerosol Air Qual. Res.* **2015**, *15* (5), 1894-1905.
4. Kamprad, I.; Goss, K.-U. Systematic investigation of the sorption properties of polyurethane foams for organic vapors. *Anal. Chem.* **2007**, *79* (11), 4222-4227.
5. Junge, C. E. *Fate of pollutants in the air and water environments*; John Wiley and Sons, Inc.: New York, 1977.
6. Pankow, J. F. Review and comparative analysis of the theories on partitioning between the gas and aerosol particulate phases in the atmosphere. *Atmos. Environ.* **1987**, *21* (11), 2275-2283.
7. Lammel, G.; Klánová, J.; Ilić, P.; Kohoutek, J.; Gasić, B.; Kovacić, I.; Škrdlíková, L. Polycyclic aromatic hydrocarbons in air on small spatial and temporal scales – II. Mass size distributions and gas-particle partitioning. *Atmos. Environ.* **2010**, *44* (38), 5022-5027.
8. Landlová, L.; Čupr, P.; Franců, J.; Klánová, J.; Lammel, G. Composition and effects of inhalable size fractions of atmospheric aerosols in the polluted atmosphere: Part I. PAHs, PCBs and OCPs and the matrix chemical composition. *Environ. Sci. Pollut. Res.* **2014**, *21* (9), 6188-6204.
9. Lei, Y. D.; Chankalal, R.; Chan, A.; Wania, F. Supercooled liquid vapor pressures of the polycyclic aromatic hydrocarbons. *J. Chem. Eng. Data* **2002**, *47* (4), 801-806.
10. Haftka, J. J. H.; Parsons, J. R.; Govers, H. A. J. Supercooled liquid vapour pressures and related thermodynamic properties of polycyclic aromatic hydrocarbons determined by gas chromatography. *J. Chromatogr. A* **2006**, *1135* (1), 91-100.
11. Odabasi, M.; Cetin, E.; Sofuoglu, A. Determination of octanol–air partition coefficients and supercooled liquid vapor pressures of PAHs as a function of temperature: application to gas–particle partitioning in an urban atmosphere. *Atmos. Environ.* **2006**, *40* (34), 6615-6625.
12. Pankow, J. F. An absorption model of gas/particle partitioning of organic compounds in the atmosphere. *Atmos. Environ.* **1994**, *28* (2), 185-188.

13. Finizio, A.; Mackay, D.; Bidleman, T.; Harner, T. Octanol-air partition coefficient as a predictor of partitioning of semi-volatile organic chemicals to aerosols. *Atmos. Environ.* **1997**, *31* (15), 2289-2296.
14. Harner, T.; Bidleman, T. F. Octanol-air partition coefficient for describing particle/gas partitioning of aromatic compounds in urban air. *Environ. Sci. Technol.* **1998**, *32* (10), 1494-1502.
15. Harner, T.; Bidleman, T. F. Measurement of octanol-air partition coefficients for polycyclic aromatic hydrocarbons and polychlorinated naphthalenes. *J. Chem. Eng. Data* **1998**, *43* (1), 40-46.
16. Dachs, J.; Eisenreich, S. J. Adsorption onto aerosol soot carbon dominates gas-particle partitioning of polycyclic aromatic hydrocarbons. *Environ. Sci. Technol.* **2000**, *34* (17), 3690-3697.
17. van Noort, P. C. M. A thermodynamics-based estimation model for adsorption of organic compounds by carbonaceous materials in environmental sorbents. *Environ. Toxicol. Chem.* **2003**, *22* (6), 1179-1188.
18. Jonker, M. T. O.; Koelmans, A. A. Sorption of polycyclic aromatic hydrocarbons and polychlorinated biphenyls to soot and soot-like materials in the aqueous environment: mechanistic considerations. *Environ. Sci. Technol.* **2002**, *36* (17), 3725-3734.
19. Goss, K.-U.; Buschmann, J.; Schwarzenbach, R. P. Determination of the surface sorption properties of talc, different salts, and clay minerals at various relative humidities using adsorption data of a diverse set of organic vapors. *Environ. Toxicol. Chem.* **2003**, *22* (11), 2667-2672.
20. Krivácsy, Z.; Kiss, G.; Ceburnis, D.; Jennings, G.; Maenhaut, W.; Salma, I.; Shooter, D. Study of water-soluble atmospheric humic matter in urban and marine environments. *Atmos. Res.* **2008**, *87* (1), 1-12.
21. Krivácsy, Z.; Kiss, G.; Varga, B.; Galambos, I.; Sárvári, Z.; Gelencsér, A.; Molnár, Á.; Fuzzi, S.; Facchini, M. C.; Zappoli, S.; Andracchio, A.; Alsberg, T.; Hansson, H. C.; Persson, L. Study of humic-like substances in fog and interstitial aerosol by size-exclusion chromatography and capillary electrophoresis. *Atmos. Environ.* **2000**, *34* (25), 4273-4281.
22. Kiss, G.; Tombácz, E.; Varga, B.; Alsberg, T.; Persson, L. Estimation of the average molecular weight of humic-like substances isolated from fine atmospheric aerosol. *Atmos. Environ.* **2003**, *37* (27), 3783-3794.
23. Kiss, G.; Varga, B.; Galambos, I.; Ganszky, I. Characterization of water-soluble organic matter isolated from atmospheric fine aerosol. *J. Geophys. Res. Atmos.* **2002**, *107* (D21), ICC 1-1-ICC 1-8.
24. Kalberer, M.; Paulsen, D.; Sax, M.; Steinbacher, M.; Dommen, J.; Prevot, A. S. H.; Fisseha, R.; Weingartner, E.; Frankevich, V.; Zenobi, R.; Baltensperger, U. Identification of

polymers as major components of atmospheric organic aerosols. *Science* **2004**, *303* (5664), 1659-1662.

25. Puxbaum, H.; Tenze-Kunit, M. Size distribution and seasonal variation of atmospheric cellulose. *Atmos. Environ.* **2003**, *37* (26), 3693-3699.

26. Després, V. R.; Alex Huffman, J.; Burrows, S. M.; Hoose, C.; Safatov, A. S.; Buryak, G.; Fröhlich-Nowoisky, J.; Elbert, W.; Andreae, M. O.; Pöschl, U.; Jaenicke, R. Primary biological aerosol particles in the atmosphere: a review. *Tellus B Chem. Phys. Meteorol.* **2012**, *64* (15598), 1-58.

27. Roth, C. M.; Goss, K.-U.; Schwarzenbach, R. P. Sorption of a diverse set of organic vapors to urban aerosols. *Environ. Sci. Technol.* **2005**, *39* (17), 6638-6643.

28. Lim, H.-J.; Turpin, B. J. Origins of primary and secondary organic aerosol in Atlanta: results of time-resolved measurements during the Atlanta Supersite Experiment. *Environ. Sci. Technol.* **2002**, *36* (21), 4489-4496.

29. Winkler, P. Die relative Zusammensetzung des atmosphärischen Aerosols in Stoffgruppen. *Meteor. Rdsch.* **1974**, *27*, 129-136.

30. Saxena, P.; Hildemann, L. M. Water-soluble organics in atmospheric particles: a critical review of the literature and application of thermodynamics to identify candidate compounds. *J. Atmos. Chem.* **1996**, *24* (1), 57-109.

31. Warneck, P. *Chemistry of the natural atmosphere*; Academic Press: San Diego, USA, 1988.

32. Rogge, W. F.; Mazurek, M. A.; Hildemann, L. M.; Cass, G. R.; Simoneit, B. R. T. Quantification of urban organic aerosols at a molecular level: identification, abundance and seasonal variation. *Atmos. Environ.* **1993**, *27* (8), 1309-1330.

33. Kubátová, A.; Vermeylen, R.; Claeys, M.; Cafmeyer, J.; Maenhaut, W. Organic compounds in urban aerosols from Gent, Belgium: characterization, sources, and seasonal differences. *J. Geophys. Res. Atmos.* **2002**, *107* (21).

34. Koop, T.; Bookhold, J.; Shiraiwa, M.; Pöschl, U. Glass transition and phase state of organic compounds: dependency on molecular properties and implications for secondary organic aerosols in the atmosphere. *Phys. Chem. Chem. Phys.* **2011**, *13* (43), 19238-19255.

35. Oliveira, T. S.; Pio, C. A.; Alves, C. A.; Silvestre, A. J. D.; Evtyugina, M.; Afonso, J. V.; Fialho, P.; Legrand, M.; Puxbaum, H.; Gelencsér, A. Seasonal variation of particulate lipophilic organic compounds at nonurban sites in Europe. *J. Geophys. Res. Atmos.* **2007**, *112* (23), 1-20.

36. Ariyasena, T. C.; Poole, C. F. Determination of descriptors for polycyclic aromatic hydrocarbons and related compounds by chromatographic methods and liquid-liquid partition in totally organic biphasic systems. *J. Chromatogr. A* **2014**, *1361*, 240-254.

37. Sprunger, L.; Proctor, A.; Acree Jr, W. E.; Abraham, M. H. Characterization of the sorption of gaseous and organic solutes onto polydimethyl siloxane solid-phase microextraction surfaces using the Abraham model. *J. Chromatogr. A* **2007**, *1175* (2), 162-173.
38. Abraham, M. H.; Ibrahim, A.; Acree Jr, W. E. Partition of compounds from gas to water and from gas to physiological saline at 310 K: linear free energy relationships. *Fluid Phase Equilib.* **2007**, *251* (2), 93-109.
39. Abraham, M. H.; Smith, R. E.; Luchtefeld, R.; Boorem, A. J.; Lou, R.; Acree Jr, W. E. Prediction of solubility of drugs and other compounds in organic solvents. *J. Pharm. Sci.* **2010**, *99* (3), 1500-1515.
40. Abraham, M. H.; Acree, W. E.; Leo, A. J.; Hoekman, D. The partition of compounds from water and from air into wet and dry ketones. *New J. Chem.* **2009**, *33* (3), 568-573.
41. Arp, H. P. H.; Schwarzenbach, R. P.; Goss, K.-U. Ambient gas/particle partitioning. 2: the influence of particle source and temperature on sorption to dry terrestrial aerosols. *Environ. Sci. Technol.* **2008**, *42* (16), 5951-5957.
42. Roth, C. M.; Goss, K.-U.; Schwarzenbach, R. P. Sorption of a diverse set of organic vapors to diesel soot and road tunnel aerosols. *Environ. Sci. Technol.* **2005**, *39* (17), 6632-6637.
43. Shahpoury, P.; Lammel, G.; Holubová Šmejkalová, A.; Klánová, J.; Příbylová, P.; Váňa, M. Polycyclic aromatic hydrocarbons, polychlorinated biphenyls, and chlorinated pesticides in background air in central Europe – investigating parameters affecting wet scavenging of polycyclic aromatic hydrocarbons. *Atmos. Chem. Phys.* **2015**, *15* (4), 1795-1805.
44. Tomaz, S.; Shahpoury, P.; Jaffrezo, J.-L.; Lammel, G.; Perraudin, E.; Villenave, E.; Albinet, A. One-year study of polycyclic aromatic compounds at an urban site in Grenoble (France): Seasonal variations, gas/particle partitioning and cancer risk estimation. *Sci. Total Environ.* **2016**, *565*, 1071-1083.
45. ACD/Labs *Absolv*, Advanced Chemistry Development, Inc., Toronto, Canada, 2015.